Electrochemical reduction of nitroso compounds: voltammetric, UV–vis and EPR characterization of *ortho*- and *meta*-nitrosotoluene derivatives

Luis J. Núñez-Vergara *, M. Bontá, J.C. Sturm, P.A. Navarrete, S. Bollo, J.A. Squella

Laboratory of Bioelectrochemistry, Faculty of Chemical & Pharmaceutical Sciences, University of Chile, P.O. Box 233, Santiago, Chile

Abstract

A comprehensive study of the electrochemical reduction, in different electrolytic media, of two nitroso compounds, i.e. *ortho*- and *meta*-nitrosotoluene derivatives has been carried out. Furthermore, UV–vis and EPR spectroscopic characterization of the one-electron reduction product from these derivatives in aprotic media is also reported. Controlled potential electrolysis (CPE) was used to generate the nitroso radical and its detection by cyclic voltammetry, UV–vis and EPR spectroscopy was achieved. In protic media (30% ethanol + 0.1 M Britton–Robinson buffer pH 5–12) both derivatives gave a reversible well-defined peak in the whole pH range on Hg in a reaction involving two electrons to give the hydroxylamine derivative. In mixed aqueous organic media (0.015 M aqueous citrate + DMF: 40:60 and 0.1 M TBAI) at pH > 8 isolation and electrochemical characterization of the nitroso radical anion was achieved. Under these experimental conditions, nitroso derivatives are reduced in a quasi-irreversible mechanism. In aprotic media (0.1 M TBAI in DMF), the nitroso radical anions decay by a dimerization, with rate constant values, k_2,: 4100 ± 52 $(M\ s)^{-1}$ and 2700 ± 28 $(M\ s)^{-1}$ for *ortho*- and *meta*- nitrosotoluene, respectively. The proposed electroreduction mechanism of the nitroso derivatives were supported by digital simulation through a DIGISIM 2.1 software version.

Keywords: Nitrosotoluene; Reduction; Polarography; Cyclic voltammetry; Radical anions; Simulation

1. Introduction

The nitroso-aromatics are an extremely important class of compound. Aromatic C-nitroso compounds can be formed as reactive intermediates in biological systems. Their formation can occur either by metabolic *N*-oxidation of arylamines, leading to methemoglobinemia, carcinogenesis, or mutagenesis or by reduction of aromatic nitro compounds, introduced into organisms as a toxin. Alternatively, some nitrocompounds can enter into organisms administered as drugs, i.e. antibiotics such as chloramphenicol, nitroimidazoles used in cancer treatment, or nitrofurans or nitrothiazoles useful as antifungicidal agents, which can be reduced to nitroso intermediates. Consequently, the reduction properties of the nitroso group are of prime importance. However, this topic has not received great attention mainly because of difficulties in the synthesis of nitroso compounds and their chemical instability. Thus, most of the literature has been devoted to nitrosobenzene [1,2]. On these lines, a good review on addition, reduction and oxidation reactions of nitrosobenzene was published some years ago by Zuman and Shah [3]. Recently our laboratory published [4] an electrochemical study on the reactivity of the nitroso radical anion generated electrochemically from nitrosobenzene with glutathione. On the other hand, electron spin resonance studies have established the intermediacy of radicals in the chemical and electrochemical reductions of nitrobenzene in aqueous and nonaqueous solvent systems [5–8].

In spite of the well-known cytotoxic properties of nitroso compounds, only a few papers [9,10] about the biological effects of nitrosotoluene derivatives have appeared.

E-mail address: lnunez@abello.dic.uchile.cl (L.J. Núñez-Vergara).

Taking into account that nitroso derivatives constitute a chemical prototype with interesting potential pharmacological and toxicological properties, a comprehensive study of the electrochemical characteristics in different electrolytic media of two nitroso compounds, i.e. *ortho*- and *meta*-nitrosotoluene derivatives, has been carried out. Furthermore, UV–vis and EPR spectroscopic characterization of the one-electron reduction product from these derivatives in aprotic media is also reported and the proposed reduction mechanisms are supported by digital simulation through a DIGISIM® 2.1 software version.

2. Experimental

2.1. Drugs and reagents

Nitrosobenzene, dimethylformamide (DMF), pro-analysis grade, and tetrabutylammonium iodide (TBAI), were purchased from Merck Laboratories (Santiago, Chile). Tetrabutylammonium hexafluorophosphate (TBAHFP) was purchased from Aldrich.

2.1.1. Preparation of nitroso derivatives

About 13.4 ml of *ortho*-nitrotoluene (15.6 g, 0.1138 mol) was added with stirring to a refluxing water + ethanol mixture (42 ml of ethanol and 24 ml of water) containing 1.5 g (0.0135 mol) of calcium chloride. 20 g finely powdered zinc was carefully added in small portions to the boiling mixture. The whole operation should take no longer than 15–20 min. The solution was filtered and the zinc oxide residues washed three times with ethanol. The clear solution obtained was added without delay to 600 ml of water + ice containing 37 g (0.2238 mol) of ferric chloride. The crude *ortho*-nitrosotoluene was filtered off and washed with cold water. The product was further purified by steam distillation, yielding 6.21 g (0.0153 mol) of pure *ortho*-nitrosotoluene. The same procedure was applied to the synthesis of *meta*-nitrosotoluene with a yield of pure product of 22.9%.

Ortho-nitrosotoluene: M.p. 72–74°C. Ref. [11]: 72–72.5°C. IR (KBr, cm^{-1}): ν_{max} 3041, 2833, 1487, 1266, 788. ^{1}H-NMR ($CDCl_3$-*d*, 300 MHz): δ 3.35 (s, 3H, Ar-CH_3), 6.3–7.6 (m, 4H, Ar-*H*).

Meta-nitrosotoluene: M.p. 50–52.8°C. Ref. [11]: 53–53.5°C. IR (KBr, cm^{-1}): ν_{max} 3052, 2920, 1388, 1220, 817. ^{1}H-NMR (300 MHz, $CHCl_3$-*d*): δ 2.5 (s, 3H, Ar-CH_3), 8–8.4 (m, 4H, Ar-*H*)

2.1.2. Polarography

Experiments were carried out in an Inelecsa® assembly PDC 1212, containing a generator/potentiostat with an A/D converter interface attached to a 12-bit microprocessor and suitable software for totally automatic control of the experiments and data acquisition. A 286 Gateway microcomputer was used for data control, acquisition, and treatment.

Operating conditions: pulse amplitude, 60 mV; potential scan, 5 mV s^{-1}; drop time, 1 s, voltage range, 0 to -2000 mV, current range, 1.25–5 μA, temperature, 25°C. All the solutions were purged with pure nitrogen for 10 min before the polarographic runs.

2.1.3. Cyclic voltammetry

Experiments were carried out in an Inelecsa® assembly similar to that described above. All cyclic voltammograms were recorded at a constant temperature of 25°C and the solutions were purged with pure nitrogen for 10 min before the voltammetric runs. The return-to-forward peak current ratio, I_{pa}/I_{pc}, for the reversible first electron transfer (the Ar-NO/Ar-$NO^{\bullet -}$ couple) was measured, the scan rate varying from 0.1 up to 100 V s^{-1}.

2.1.4. Electrodes

A Metrohm hanging mercury drop electrode (HMDE) with a drop surface of 1.90 mm^2 (VC) and a dropping mercury electrode (DME) (DPP and tast polarography) were used as the working electrodes and a platinum wire as the counter electrode. All potentials were measured against a saturated calomel electrode.

2.1.5. Methods

The experimental I_{pa}/I_{pc} ratios were calculated according to the procedure of Nicholson and Shain, using individual cyclic voltammograms [12].

Kinetic reaction orders for the nitroso radical anion were quantitatively assayed for first and second-order coupled reactions according to a previously published study [13].

2.1.5.1. Controlled potential electrolysis. CPE was carried out either on a platinum coil electrode or a glassy carbon electrode at -1000 mV in anhydrous acetonitrile containing 0.1 M TBAHFP as supporting electrolyte. Oxygen was removed by pure, dry pre-saturated nitrogen. A three-electrode circuit with a $Ag \mid AgCl \mid KCl_{sat}$ electrode was used as the reference. A Wenking potentiostat model POS 88 was used to electrolyze nitrosotoluene (NOT) derivatives.

2.1.5.2. UV–vis spectroscopic studies. In order to obtain further information on the mechanism, mainly on the progress of the electrolysis, a UNICAM UV-3 spectrophotometer was used. UV–vis spectra were recorded in the 220–800 nm range at different intervals. Acquisition and data treatment were carried out with the VISION 2.11 software. An electrolytic cell of our own construction [14], based on a 1 cm UV cuvette, with a

platinum coil as the working electrode was used for the in situ generation of the reduction species. The electrolysis was conducted under constant stirring, which was stopped before each measurement.

2.1.5.3. EPR measurements. The nitroso radical anion from nitrosotoluene derivatives was generated in situ in the EPR cavity by electrochemical reduction (-1000 mV) on a platinum wire at room temperature (r.t.). The Wilmed WG-810 flat electrolytic cell (Wilmed Glass, Route 40 and Oak Road, Buena, NJ 08310 USA) includes a pair of platinum electrodes and an $Ag \mid AgCl \mid KCl_{sat}$ reference electrode. A 5 mM solution of the nitrosotoluene derivative containing 0.1 M TBAHFP in acetonitrile, was purged with nitrogen for 10 min, then reduced and immediately its EPR spectrum was recorded in the microwave band X (9.67 GHz) in a Bruker ECS 106 spectrometer. Hyperfine splitting constants were estimated to be accurate within 0.05 G.

2.1.6. Protic media

All compounds were dissolved in 0.1 M Britton–Robinson buffer + ethanol: 70/30 to obtain the final concentration, which varied between 0.1 and 1 mM.

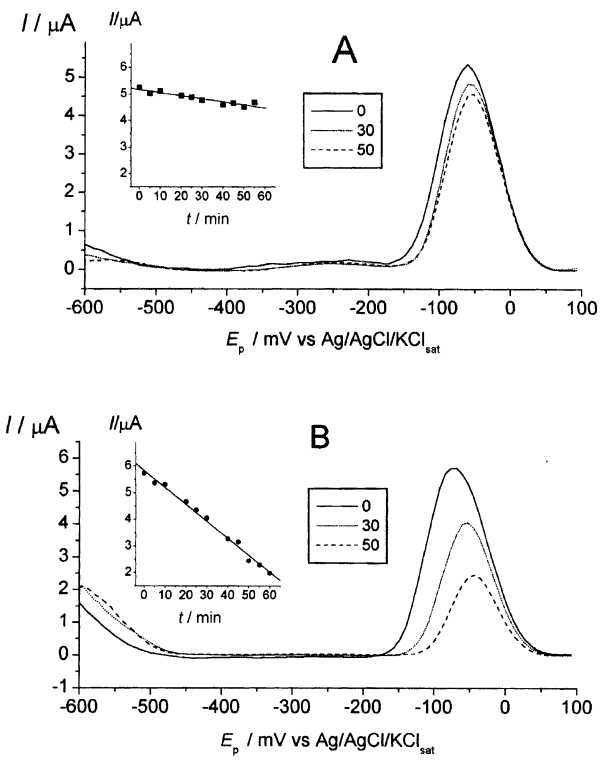

Fig. 1. Decay of the current peak of: (A) *o*-NOT and (B) *m*-NOT derivatives at different aging times. Concentration: 1 mM in 0.1 M Britton–Robinson buffer + ethanol: 70/30, pH 7.

2.1.7. Mixed media

From preliminary studies to obtain the optimal mixed media we have selected the following composition: 0.015 M aqueous citrate + DMF: 60/40 and 0.1 M TBAI at pH 9.0. All derivatives were previously dissolved in DMF.

2.1.8. Aprotic media

All compounds were dissolved in DMF containing 0.1 M TBAI. The final concentration varied between 0.1 and 1 mM.

2.2. pH in mixed media

pH measurements were corrected according to the following expression [15]: $pH^* - B = \log U_H^0$, where pH* equals $-\log a_H$ in the mixed solvent, B is the pH meter reading and the term $\log U_H^0$ is the correction factor for the glass electrode. This factor was calculated for different mixtures of DMF and aqueous solvent, according to a previously reported procedure [15] and applied to our experimental pH determinations.

2.3. Simulations

CV curves were recorded with a BAS CV-50W electrochemical system with a controlled growth mercury electrode (CGME), linked to a Gateway 2000 PC for acquisition and data processing. A three electrode cell containing an HMDE as the working electrode, an $Ag \mid AgCl \mid KCl_{sat}$ electrode supplied with a bridge for mixed solvents as the reference electrode and a platinum wire as an auxiliary electrode. Simulated CV curves were obtained using software DIGISIM® 2.1 CV simulator for Windows. Software was run using a Gateway 2000 PC.

3. Results and discussion

3.1. Reduction in protic media of o-nitrosotoluene (o-NOT) and m-nitrosotoluene (m-NOT) derivatives

3.1.1. Polarography

Both compounds were relatively unstable in solution the *m*-NOT derivative being more unstable than the *o*-NOT derivative. In Fig. 1 we can observe the decay of the polarographic signal with time showing the instability of both compounds in solution. Because of the instability of the nitroso derivatives, fresh solutions were prepared for each set of experiments.

At $pH < 5$ the nitroso derivatives did not produce a polarographic peak or wave because their reduction was masked by the mercury oxidation in 0.1 M Britton–Robinson buffer + ethanol: 70/30. However, at $pH > 5$ both derivatives exhibited similar polarographic

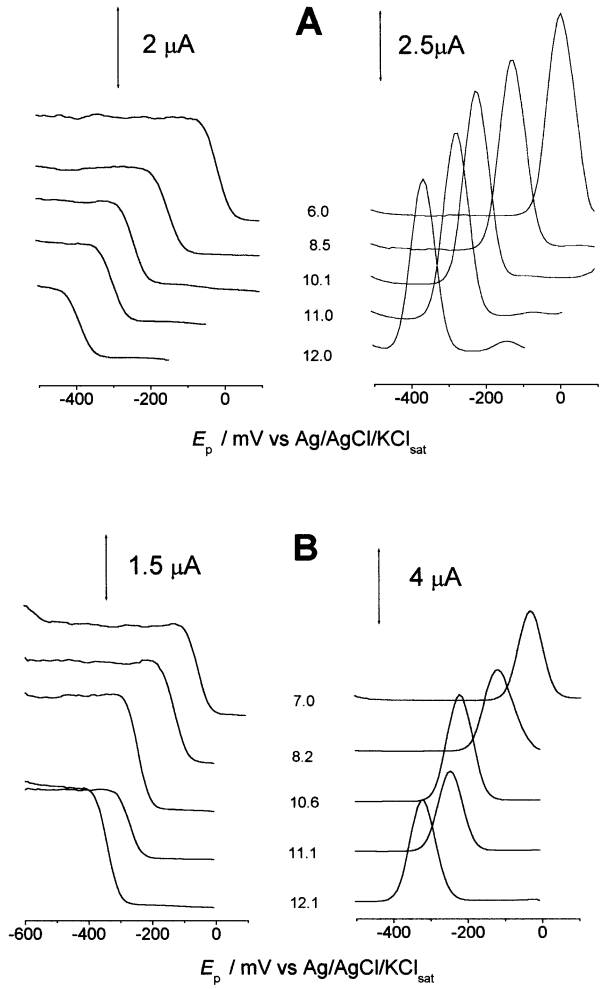

Fig. 2. Tast and DP polarograms of: (A) *o*-NOT and (B) *m*-NOT derivatives at different pH values in a protic medium. Concentration: 1 mM.

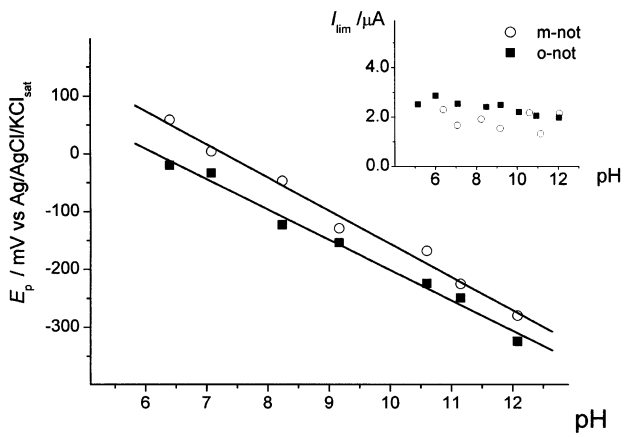

Fig. 3. Potential peak and limiting current (insert) dependence on pH for a 1 mM solution of *o*-NOT and *m*-NOT derivatives in 0.1 M Britton–Robinson buffer + ethanol: 70/30.

behavior with a single well-defined peak in the DPP mode. As can be seen in Fig. 2, the peaks are shifted to more negative potentials with increasing pH within the range between pH 5 and 12.

The E_{pc} plots show a single linear segment with pH for the whole range studied, i.e. pH 5–12, for both derivatives. These linear dependences are shown in Fig. 3. In tast polarography mode, the compounds presented a similar dependence between $E_{1/2}$ and pH. Furthermore, in the insert of Fig. 3, we can observe that the limiting currents practically remain constant in the whole pH range. Similar behavior for the peak area with pH was observed, indicating its independence of both the kinetic and the reduction mechanisms.

Applying Tomes criterion [16] an $|E_{3/4} - E_{1/4}|$ experimental value of 35 ± 3 at different pH values was determined, which was consistent with the theoretical value of 28 mV, which indicated that the reduction process had a reversible character and involved 2 electrons. Consequently, the reduction of both NOT derivatives takes place according to:

$$\text{Ar-NO} + 2e^- + 2H^+ \leftrightarrow \text{Ar-NHOH} + H_2O \quad (1)$$

m-NOT is reduced at less negative potentials at approximately 20 mV in the whole pH range. A plausible explanation for these results could be ascribed to the different electron-donating and mesomeric properties of

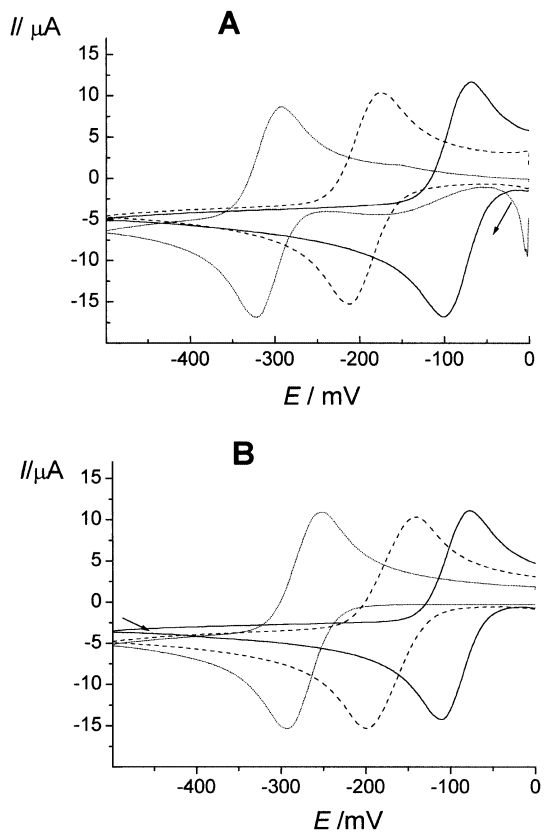

Fig. 4. Effect of pH on the cyclic voltammograms of: (A) *o*-NOT and (B) *m*-NOT in a protic medium. pH 7.5 (—), pH 9.1 (– – –), pH 11 (……). Sweep rate: 1 V s^{-1}. Concentration: 1 mM.

the methyl group on the electron density of the nitroso moiety in the *ortho*-position compared with the *meta*-position.

Electrocapillary curve analyses at different concentrations and pH values indicated that the zero-charge potential was about -300 mV. Moreover, comparison of the electrocapillary curves between buffer and nitroso compounds plus buffer solutions reveals that there is no adsorption involved.

A comparison of tast polarograms of solutions at the same concentrations and pH of NOT derivatives with those of nitrosobenzene showed that the ratio of their limiting currents was close to 1, confirming that the reduction of these NOT derivatives is also due to a 2-electron, 2-proton overall mechanism as is that of nitrosobenzene.

3.1.2. Cyclic voltammetry

In protic medium at pH < 7 no signals were observed. At pH > 7 both derivatives gave a reversible well-defined peak in the pH range between 7.4 and 12. Potentials were shifted to more negative values as the pH increased (Fig. 4).

The reduction process corresponds to the reduction of the nitroso group to the hydroxylamine derivative, as was shown in Eq. (1).

The calculated ΔE_p values for these couples are close to 30 mV, confirming that the reduction process for both derivatives in this medium involved the transfer of two electrons. A similar conclusion was obtained after the analyses of the cathodic peak half-widths, since the experimentally calculated values were close to 30 mV, consistent with the theoretical value of 28 mV for a

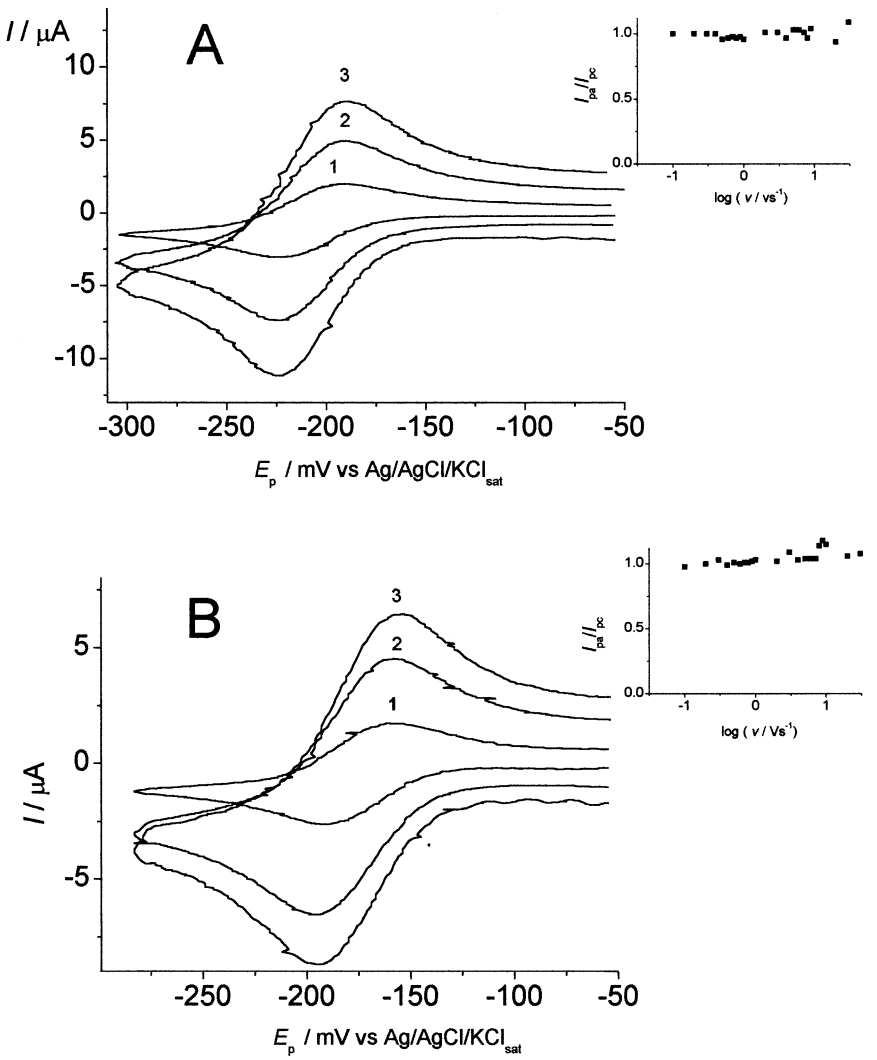

Fig. 5. Isolated reversible couples of : (A) *o*-NOT and (B) *m*-NOT at different sweep rates (1 = 0.1, 2 = 0.5, 3 = 1.0 V s^{-1}) at pH 9 in a protic medium. Concentration: 1 mM. Inset: Dependence of I_{pa}/I_{pc} ratio with log v.

reversible reduction involving 2 electrons. Furthermore, the fact that only one peak appears for the two-electron transfer implies that the transfer of the second electron is easier than the first one.

To investigate the reduction mechanism, the reversibility of the couples was analyzed at pH 9. As can be seen from Fig. 5, in parallel with an increasing sweep rate, an increase of both cathodic and anodic currents was obtained, but the I_{pa}/I_{pc} ratio was independent of the logarithm of sweep rate ($I_{pa}/I_{pc} = 1$). The above result indicates that the reduction process is reversible. Also, the cathodic peak potentials did not vary with the logarithm of sweep rate.

On the other hand, the $I_{pc}/v^{1/2}$ ratio became independent of the sweep rate, indicating that adsorption processes do not complicate the reduction on the electrode surface. Furthermore, the cathodic currents exhibited a linear dependence with $v^{1/2}$. Consequently, we obtained a linear relation for log I_p versus log v with slope values close to 0.5 suggesting a diffusion controlled process.

3.2. Reduction in mixed media of o-NOT and m-NOT derivatives

3.2.1. Polarography

The following mixed medium containing 0.015 M citrate + DMF: 40/60 and 0.1 M TBAI was selected. At pH < 8, the nitroso derivatives did not show any signal at the DME. However, at pH > 8 both derivatives were reduced following similar polarographic behavior with a single well-defined peak in the DPP mode. The peaks were shifted to more negative potentials with increasing pH within the range between pH 8 and 12 (Fig. 6). A linear dependence of E_{pc} with pH in the range between pH 8 and 12 for both derivatives was observed. In Fig. 7 we can observe the linear relation between the cathodic peak potential with pH for both derivatives. In tast polarography mode, the compounds presented a similar dependence between $E_{1/2}$ and pH. Furthermore, as can be observed in the insert of Fig. 7, the limiting currents were relatively pH-independent.

Applying Tomes criterion, a $|E_{3/4} - E_{1/4}|$ experimental value of 45.5 ± 4 mV at the different pH values was

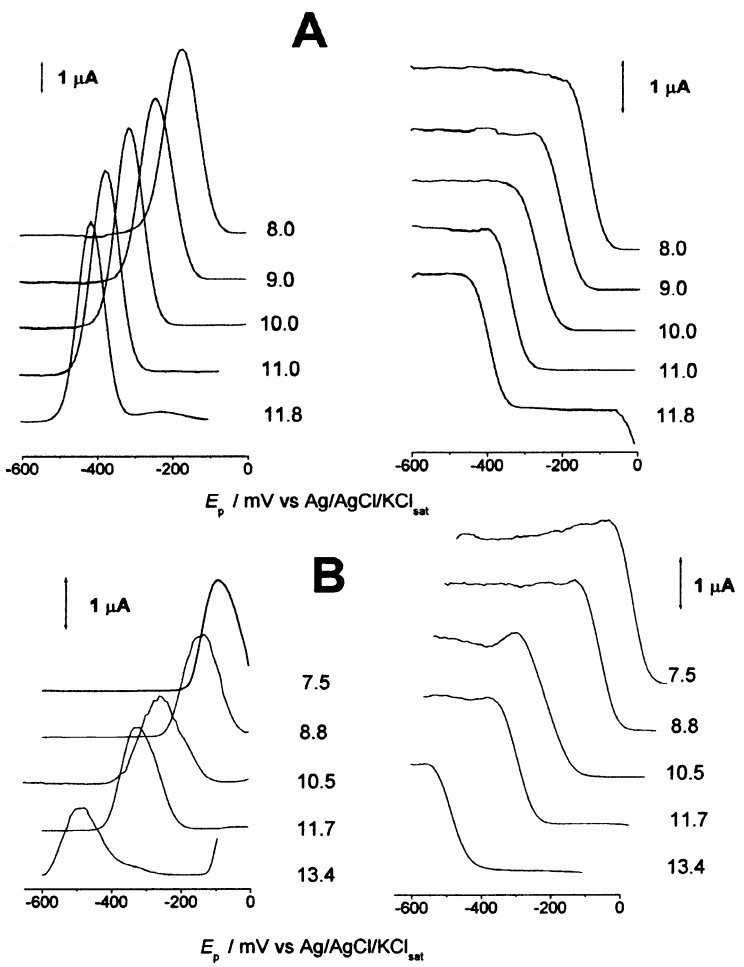

Fig. 6. Tast and DP polarograms of: (A) *o*-NOT and (B) *m*-NOT at different pH values in a mixed medium. Concentration: 1 mM.

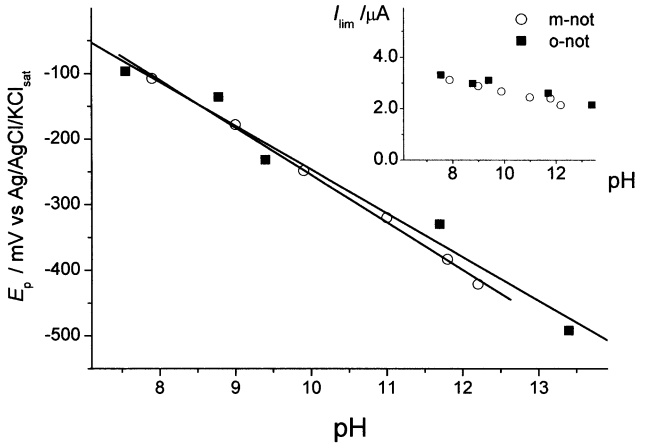

Fig. 7. Potential peak and limiting current (insert) dependence on pH for a 1 mM solution of *o*-NOT and *m*-NOT derivatives in a mixed medium.

determined, which is significantly different from the theoretical value of 28 mV for a reversible process involving 2 electrons, but closer to the 56 mV value for a 1-electron transfer. Consequently, both NOT derivatives are reduced to the corresponding nitroso radical anion involving 1 electron according to the following reaction:

$$\text{Ar-NO} + \text{e}^- \leftrightarrow \text{Ar-NO}^{\bullet -} \quad (2)$$

3.2.2. Cyclic voltammetry

Cyclic voltammetry was carried out in the same electrolytic medium as the polarographic experiments. At pH higher than pH 9, well-resolved couples for both derivatives appeared. The ΔE_p value for the couples was about 80 ± 10 mV (mean value obtained at pH 9 for both compounds and at different sweep rates), which increased in parallel with the increase of the sweep rate. On the other hand, the cathodic peak width had a value of 72 ± 15 mV. Both results indicate that the process corresponds to reduction of the nitroso derivatives to give the nitroso radical anion, involving the 1 electron transfer according to Eq. (2).

The I_{pa}/I_{pc} ratios proved to be independent of the logarithm of sweep rate, but were lower than unity, probably due to the existence of a parallel surface heterogeneous protonation. Adsorption processes were not detected because the $I_{pc}/v^{1/2}$ ratio was independent of the logarithm of sweep rate. Also, the cathodic peak current behaved linearly with $v^{1/2}$ confirming that the electrode process was diffusion controlled. The above results were consistent with the linear dependences of $\log I_p$ versus $\log v$. The experimental slope values from such plots were: 0.5084 (corr. coeff. 0.9985) and 0.5210 (corr. coeff. 0.9990) for the *o*-NOT and the *m*-NOT derivatives, respectively. Finally, the cathodic peak potential values depended linearly on the logarithm of sweep rate. Thus, from the above-described results the reduction in this medium does not fulfil the electrochemical criteria for a system which is completely reversible, therefore the electron transfer corresponds to a quasi-reversible process.

3.3. Reduction in aprotic media of o-NOT and m-NOT derivatives

3.3.1. Polarography

In this medium (100% dimethylformamide + 0.1 M TBAI) both in DPP mode and tast polarography, the compounds exhibited two signals. However, because of low resolution and reproducibility of the signals their characterization was not possible.

3.3.2. Cyclic voltammetry

Both derivatives exhibited a prewave followed by a reversible couple. Prewaves appeared at $E_{pc} = -772$ and $E_{pc} = -808$ mV; the reversible couples had the following peak potential values: $E_{pa} = -854$ and $E_{pc} = -932$ mV and $E_{pa} = -841$ and $E_{pc} = -921$ mV for *o*-NOT and *m*-NOT, respectively (Fig. 8 A and B). The addition of ethanolic NaOH solution produced a decrease of the intensity of the prewaves. Thus, a 4.8 mM NaOH concentration permitted the observation of a well-resolved reversible couple for *o*-NOT (Fig. 8A, curve 3). An equivalent effect was achieved at a 3.2 mM NaOH concentration for the *m*-NOT derivative (Fig. 8B, curve 3). A possible explanation for the appearance of this prewave could be the adduct formation between the oxygen atom of the aromatic nitroso group and a proton provided by the presence of water in the medium. A similar effect has been previously described by Kwiatek and Kalinowski [18] for the case of nitrobenzene.

Because the addition of ethanolic NaOH suppressed the prewaves, the electrochemical characterization of the reversible couples was achieved.

The experimental ΔE_p average values were 79 ± 2 mV, which is relatively close to the theoretical value of 60 mV for a monoelectronic transfer [13]. The reduction peak potential values for both nitroso derivatives were very close, i.e. -921 and -932 mV for *o*-NOT and *m*-NOT, respectively.

The independence of the $I_{pc}/v^{1/2}$ ratio of the logarithm of sweep rate shows that no adsorption processes are present, complicating the reduction process. Also, the cathodic peak current exhibited a linear dependence on $v^{1/2}$, confirming that the electrode process is diffusion controlled. A similar conclusion can be obtained from the linear dependences of $\log I_p$ versus $\log v$. The experimental slope values from such plots were 0.488 (corr. coeff. 0.9992) and 0.501 (corr. coeff 0.9995) for the *o*-NOT and the *m*-NOT derivatives, respectively.

From the dependence of the I_{pa}/I_{pc} ratio with the logarithm of the sweep rate, it is clear that the 1

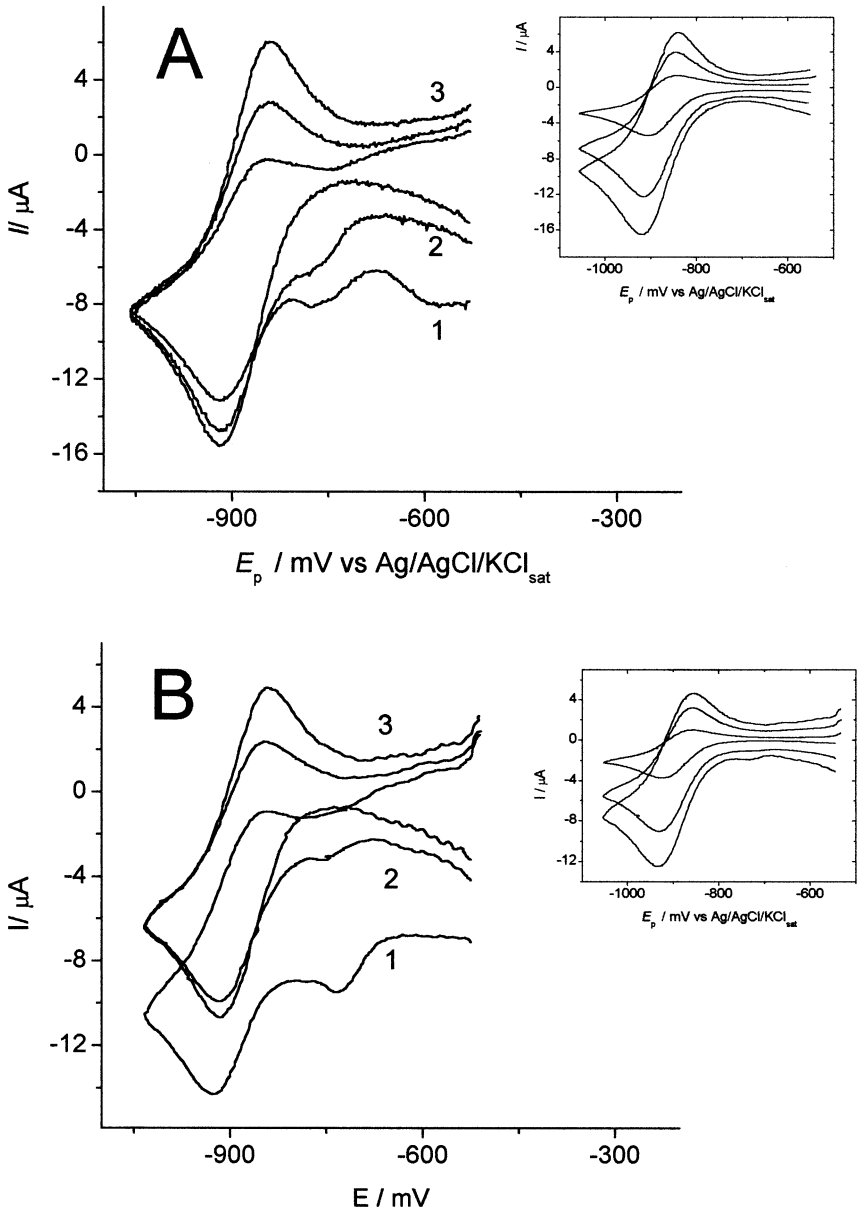

Fig. 8. Effect of the addition of NaOH on the cyclic voltammograms in an aprotic medium of (A) 1 mM *o*-NOT: (1) no addition of NaOH (2) 2.4 mM NaOH (3) 4.8 mM NaOH; (B) 1 mM *m*-NOT: (1) no addition of NaOH (2) 1.6 mM NaOH (3) 3.2 mM NaOH. Inset: Isolated reversible couples at different sweep rates (0.1, 0.5, 1.0 V s^{-1}) after the addition of 3.2 mM NaOH.

electron transfer to give the nitroso radical anion, is followed by an irreversible chemical reaction, i.e. an ECi type of mechanism, which can be represented as:

$$Ox + e^- \leftrightarrow Red$$

$$Red \rightarrow Products$$

As predicted by Olmstead et al. [17] for a second order reaction, the I_{pa}/I_{pc} ratio decreases with increasing concentration of the electroactive species. Furthermore, the cathodic peak potential also depends on the nitrosotoluene concentration and sweep rate, with $dX_{pc}/d \log c$ and $dE_{pc}/d \log v$ values varying between 19 ± 3 mV. These values are in agreement with the theoretical value of 19.5 mV for an EC_i process where the chemical step follows second order kinetic [13]. The second-order rate constants were assessed from single voltammograms, according to Olmstead et al. [17] from the following relationship:

$$\log \omega = \log (k_2 c_0 \tau)$$

Confirming the second-order character of the following chemical reaction, plots of the kinetic parameter, ω, versus the time constant, τ, were linear for both derivatives. (average corr. coeff. 0.9997).

Table 1
Calculated values of second order decay constants (k_2) and half-lives ($t_{1/2}$) at 1 mM concentration for the corresponding Ar-NO/Ar-NO$^{\bullet-}$ couples in aprotic media

	k_2/M^{-1} s^{-1}	$t_{1/2}$/s	Corr. coeff.
	Dismutation process		
ortho-Nitrosotoluene	25 000	0.039	0.9888
meta-Nitrosotoluene	21 000	0.046	0.9932
	Dimerization process		
ortho-Nitrosotoluene	4100	0.24	0.9923
meta-Nitrosotoluene	2700	0.37	0.9897

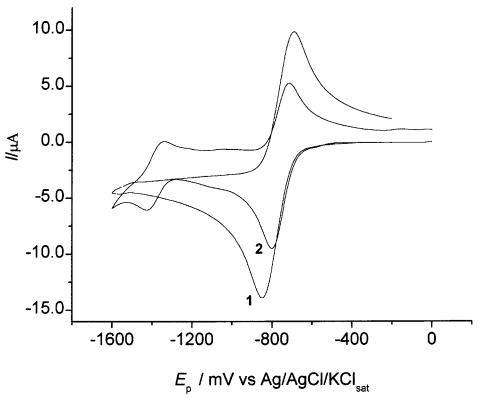

Fig. 9. Time-course of CPE of 3.1 mM *o*-NOT solution followed by cyclic voltammetry. 1 = 0 min, 2 = 10 min. Sweep rate: 0.1 V s^{-1}.

From plots of the kinetic parameter, ω, versus the time constant, τ, assuming either dimerization or dismutation processes, the rate constants were calculated for the NOT derivatives, which can be seen in Table 1. To decide which type of decay process adjusted better to the real mechanism, a simulation procedure was used. However, from this preliminary determination, independent of the type of decay, the radical corresponding to the *m*-NOT derivative appears to be more stable than that of *o*-NOT.

3.3.3. Controlled potential electrolysis

The electroanalytical behavior of *o*-NOT and *m*-NOT is very similar, in spite of changing the DMF solvent to acetonitrile, but in order to carry out the electrolysis experiment we chose acetonitrile because DMF shows a strong absorption band below 300 nm which interfered with the UV determination.

CPE of nitrosotoluene derivatives in acetonitrile to obtain the nitroso radical anion were carried out. Thus, electrolysis on a platinum electrode was performed and cyclic voltammetric curves were recorded at several intervals. In Fig. 9, cyclic voltammograms corresponding to the *o*-NOT derivative under two different sets of experimental conditions are shown. As can be seen from this figure, before the electrolysis (curve 1), only a reversible couple corresponding to the nitroso radical anion formation is observed, with the following potentials: $E_{pc} = -851$ and $E_{pa} = -692$ mV. However, after 10 min of electrolysis, together with the first reduction process, a second reversible couple (curve 2) at $E_{pc} = -1.428$ and $E_{pa} = -1.338$ mV appeared. This latter couple could correspond to the azoxy derivative formation [2,4]. Similar results were obtained for the *m*-NOT derivative.

From our experimental data and other data in the literature [2–4] it can be concluded that the chemical step in the reduction of nitrosotoluene derivatives in acetonitrile corresponds to a dimerization (see next section) with elimination of water and presumably through participation of protons from the solvent to give the azoxy derivatives (second reversible couple). The mechanism can be summarized by the following equations:

$$\text{Ar-NO} + e^- \leftrightarrow \text{Ar-NO}^{\bullet -} \quad (3)$$

$$2\text{Ar-NO}^{\bullet -} + 2H^+ \rightarrow \text{Ar-N(O)=N-Ar} + H_2O \quad (4)$$

3.3.4. UV–vis spectroscopic studies

UV–vis curves on the time-course of electrolysis for both derivatives were recorded at different intervals in acetonitrile. Fig. 10 shows how the original absorptions at $\lambda_{max} = 288$ and $\lambda_{max} = 314$ nm corresponding to *o*-NOT decreased during CPE. On the other hand, the intensity of the trough at 246 nm increased. An isobestic point at 268 nm was also observed. For the case of the *m*-NOT derivative, the original UV bands at 284 and 305 nm also decreased, concomitantly with the increase of the trough at 244 nm during CPE. These results show a significant diminution in the original λ_{max}, which indicates that reduction of the nitroso group occurred. Furthermore, as a consequence of the electrolysis a significant change in the color of the

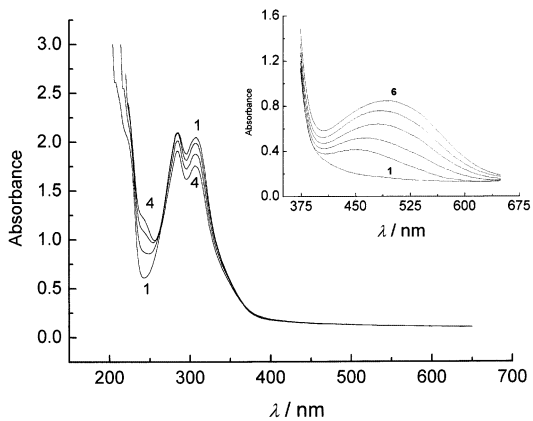

Fig. 10. Time-course of CPE of 0.2 mM *m*-NOT solution followed by UV–vis spectra. 1–4 = 30 min. Inset: Visible spectrum corresponding to the nitroso radical anion formation from a 4.4 mM *m*-NOT solution. 1–6 = 0–12 min.

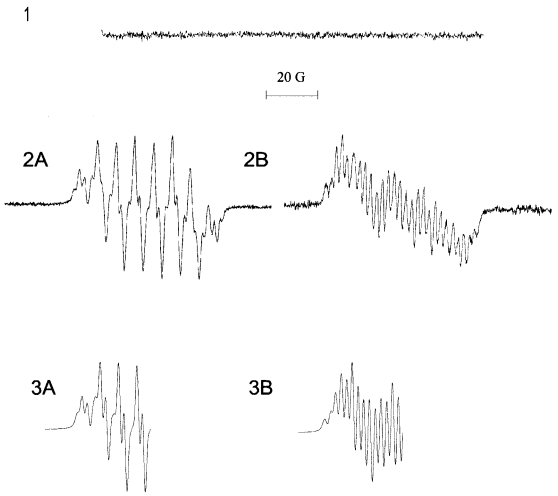

Fig. 11. Experimental EPR spectra of: (1) 0.1 M TBAHFP in acetonitrile (2) nitroso radical anion electrochemically generated from a 5 mM concentration of both *m*-NOT (2A) and (2B) *o*-NOT derivatives (3) Simulated spectra of *m*-NOT (3A) and (3B) *o*-NOT radical anions.

solution, from light green to violet, occurred. Curiously, this change was not observed in the spectra. To show the appearance of changes in the visible spectrum, the initial concentration of NOT derivatives was increased by 20 times the concentrations required to observe changes in the original bands. Thus, as can be seen from Fig. 10, (inset, spectra 1–6), concomitantly with the increase of the time-course of electrolysis, a visible band with a maximum at 498 nm (460 nm for *o*-NOT) was observed. These facts indicate that there is a new species in solution, i.e. the nitroso radical anion.

3.3.5. Electron paramagnetic resonance experiments

The electrochemical reduction of *o*-NOT and *m*-NOT to the corresponding nitroso radical anions and its detection by EPR was carried out in acetonitrile. The experimental spectra of these radicals are shown in Fig. 11 (curves 2A and B). The interpretation of the EPR spectra by means of a simulation process led us to the determination of the coupling constants for all magnetic nuclei (Table 2). Furthermore, the simulated spectra (Fig. 11, curves 3A and B) show good agreement with the hyperfine constant assignments. For comparison purposes, the hyperfine coupling constants for nitrosobenzene are also shown.

4. Simulation of cyclic voltammograms

In this section the confirmation of the previously proposed redox mechanisms is carried out through the use of the CV simulation DIGISIM® software in the different electrolytic media. The uses of this simulator to study nitrocompounds have been previously reported [19].

4.1. Simulation in protic media

In aqueous media, the reduction of the nitroso group exhibited a single signal, involving the two electron and two proton transfers in four stages, which are coupled to give this one signal. To achieve an adequate simulation, we postulate a mechanism according to the following equations:

$$\mathrm{ArNO} + \mathrm{e}^- \leftrightarrow \mathrm{ArNO}^{-\bullet} \quad (5)$$

$$\mathrm{ArNO}^{-\bullet} + \mathrm{H}^+ \leftrightarrow \mathrm{ArNOH}^{\bullet} \quad (6)$$

$$\mathrm{ArNOH}^{\bullet} + \mathrm{e}^- \leftrightarrow \mathrm{ArNOH}^- \quad (7)$$

$$\mathrm{ArNOH}^- + \mathrm{H}^+ \leftrightarrow \mathrm{ArNHOH} \quad (8)$$

Consequently, according to the requirements of the simulator software, the following parameters must be considered: electron transfer heterogeneous constant, k_s, standard potential, $E°$, electron transfer coefficient, α, equilibrium constant, K_{eq}, rate constants, k_f and k_b for the chemical reaction, diffusion coefficient and concentration of the involved species. To assign the electron transfer reaction constants, the reversibility criteria for cyclic voltammetry were taken into account [13]. Thus, a reversible cyclic voltammogram is produced when, $k_s/\mathrm{cm\ s^{-1}} > 0.3\ (nv)^{1/2}$, in contrast for an irreversible voltammogram $k_s/\mathrm{cm\ s^{-1}} < 2 \times 10^{-5}\ (nv)^{1/2}$. For the simulation in this medium we have selected the following parameters:

o-NOT:

First electrochemical step: $E° = -0.22$ V, $\alpha = 0.5$, $k_s = 1 \times 10^4$ cm s^{-1}

Table 2
Hyperfine coupling constant values for the Ar-NO$^{\bullet -}$ radical anions electrochemically generated from different nitroso aryl derivatives

Derivative	a^N/G	$a_o{}^H$/G	a_o^H/G	a_m^H/G	a_m^H/G	$a_p{}^H$/G	a_{CH3}^H/G
ortho-Nitrosotoluene	8.72	–	2.30	1.28	1.28	3.85	2.30
meta-Nitrosotoluene	8.20	4.00	3.00	–	1.41	4.00	1.02
Nitrosobenzene [a]	7.64	3.82	2.91	1.00	1.00	3.82	–

[a] Taken from Ref. [4].

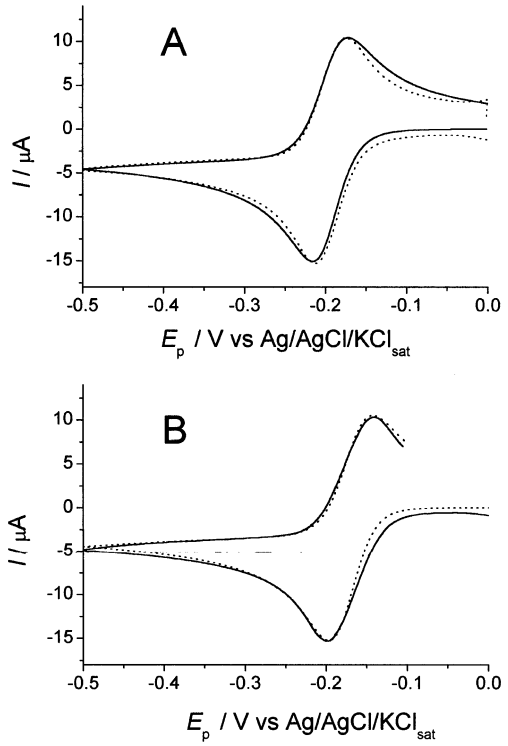

Fig. 12. Comparison of experimental (—) and simulated (...) CVs from 5 mM nitroso derivative solutions: (A) *o*-NOT (B) *m*-NOT in a protic medium.

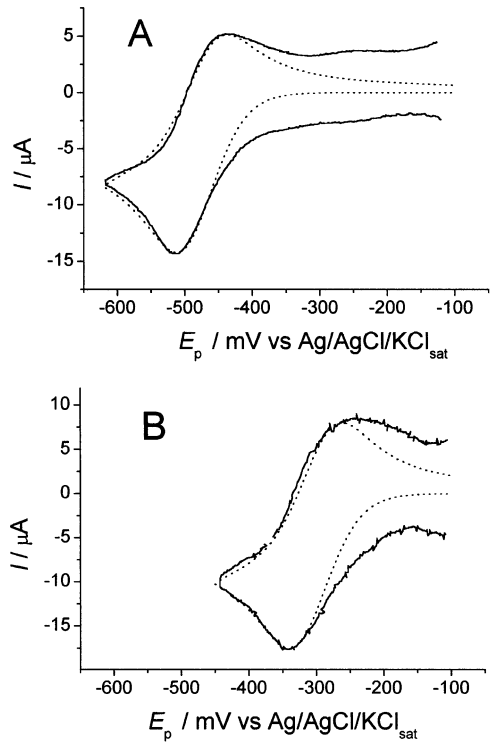

Fig. 13. Comparison of experimental (—) and simulated (...) CVs from 5 mM nitroso derivative solutions: (A) *o*-NOT (B) *m*-NOT in a mixed medium.

First chemical step: $K_{eq} = 1$, $k_f = 1 \times 10^6$, $k_b = 1 \times 10^6$
Second electrochemical step: $E° = -0.17$ V, $\alpha = 0.5$, $k_s = 1 \times 10^4$ cm s^{-1}
Second chemical step: $K_{eq} = 100$, $k_f = 5 \times 10^5$, $k_b = 5000$

m-NOT:
First electrochemical step: $E° = -0.23$ V, $\alpha = 0.5$, $k_s = 1 \times 10^4$ cm s^{-1}
First chemical step: $K_{eq} = 1$, $k_f = 1 \times 10^6$, $k_b = 1 \times 10^6$
Second electrochemical step: $E° = -0.11$ V, $\alpha = 0.5$, $k_s = 1 \times 10^4$ cm s^{-1}
Second chemical step: $K_{eq} = 100$, $k_f = 5 \times 10^5$, $k_b = 5000$

For the assignments of these parameters, we have considered that the electrochemical steps were fast or reversible, accounting for the Ar-NO/Ar-NHOH couple, which experimentally is reversible.

As can be seen from Fig. 12, the simulated CVs are coincident with the experimental CVs thus supporting the assumption of a mechanism involving the 2-electrons 2-protons transfer in four different stages, the second electron transfer being easier than the first one.

4.2. Simulation in mixed media

For this simulation, the reduction of nitroso group to the corresponding nitroso radical anion followed by a protonation of the radical was considered according to the following equations:

$$Ox + e^- \leftrightarrow Red$$

$$Red + H^+ \rightarrow C$$

For the simulation in this media we have selected the following parameters:

o-NOT:
Electrochemical step: $E° = -0.475$ V, $\alpha = 0.5$, $k_s = 0.3$ cm s^{-1}
Chemical step: $K_{eq} = 1 \times 10^3$, $k_f = 1 \times 10^3$, $k_b = 1$

m-NOT:
Electrochemical step: $E° = -0.3$ V, $\alpha = 0.5$, $k_s = 0.3$ cm s^{-1}
Chemical step: $K_{eq} = 1 \times 10^3$, $k_f = 1 \times 10^3$, $k_b = 1$

Fig. 13 shows the agreement between experimental and simulated CVs in this medium, which allows us to conclude that the surface heterogeneous protonation must be fast and irreversible in character, so that the radicals do not reach 100% reversibility in the sweep rate studies, deactivating the radicals in the negative sweep.

4.3. Simulation in aprotic media

In this medium, an EC_i mechanism type was considered, i.e a first reaction involving a one-electron transfer

accounting for the nitroso radical anion followed by an irreversible chemical reaction, according to:

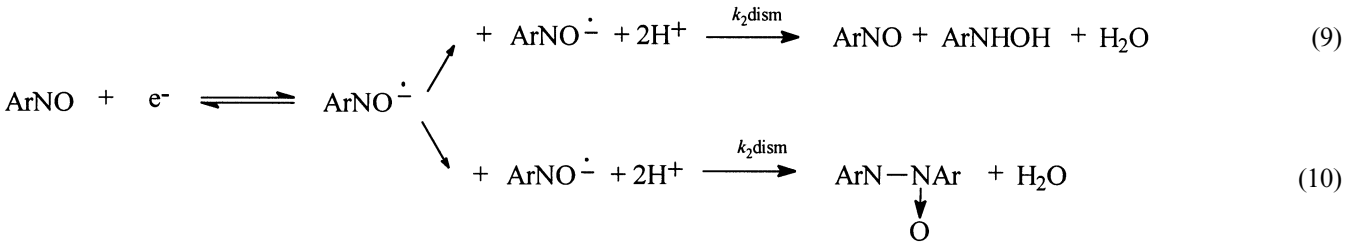

Kinetic constants (considering either the dimerization or dismutation reaction) were calculated from plots of the kinetic parameter, ω, versus the time constant, τ, at a sweep rate of 1 V s^{-1}. For dimerization or dismutation we have used the theoretical curves described in Refs. [17] or [20], respectively.

For the dimerization reaction the following parameters were selected:

o-NOT:

Electrochemical step: $E° = -0.89$ V, $\alpha = 0.5$, $k_s = 1 \times 10^4$ cm s^{-1}

Chemical step: $K_{eq} = 4.08 \times 10^3$, $k_f = 4.08 \times 10^3$, $k_b = 1$

m-NOT:

Electrochemical step: $E° = -0.9$ V, $\alpha = 0.5$, $k_s = 1 \times 10^4$ cm s^{-1}

Chemical step: $K_{eq} = 2.76 \times 10^3$, $k_f = 2.76 \times 10^3$, $k_b = 1$

For a dismutation reaction the following parameters were selected:

o-NOT:

Electrochemical step: $E° = -0.89$ V, $\alpha = 0.5$, $k_s = 1 \times 10^4$ cm s^{-1}

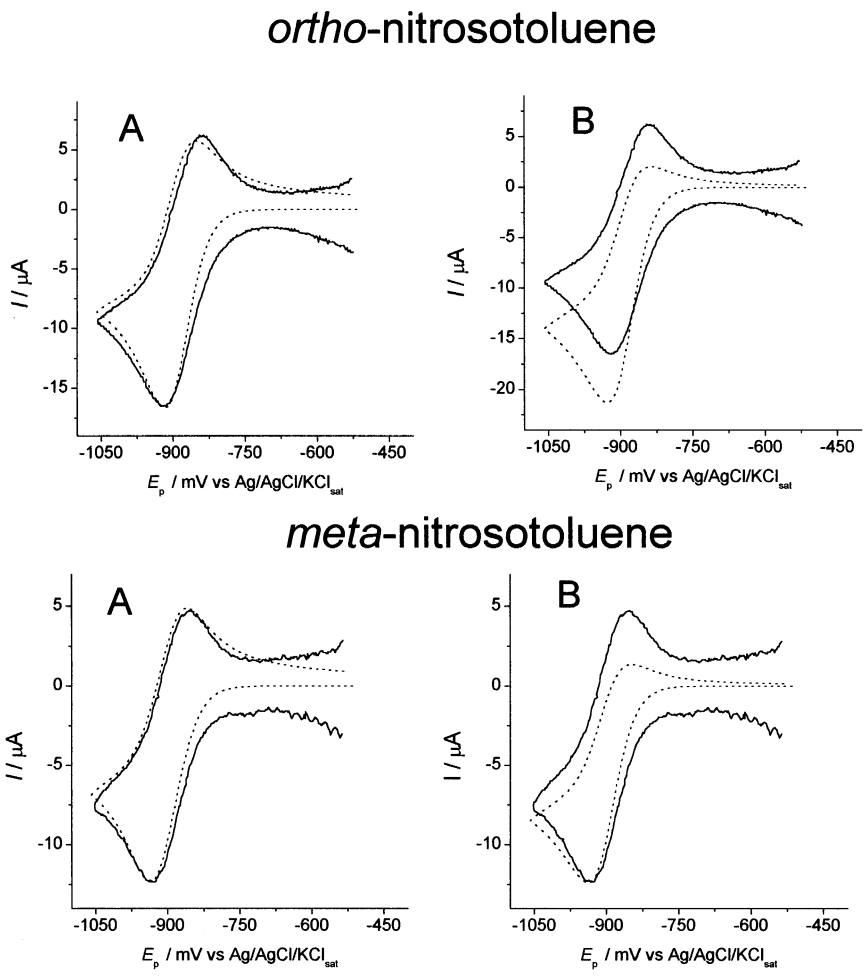

Fig. 14. Comparison of experimental (—) and simulated (…) CVs from 5 mM nitroso derivative solutions in an aprotic medium: (A) dimerization, (B) dismutation.

Chemical step: $K_{eq} = 2.52 \times 10^4$, $k_f = 2.54 \times 10^4$, $k_b = 1$

m-NOT:

Electrochemical step: $E° = -0.9$ V, $\alpha = 0.5$, $k_s = 1 \times 10^4$ cm s^{-1}

Chemical step: $K_{eq} = 2.15 \times 10^4$, $k_f = 2.15 \times 10^4$, $k_b = 1$

A comparison of both experimental and simulated CVs for the different processes is shown in Fig. 14. Our results agree very well with an irreversible chemical reaction corresponding to a dimerization reaction.

5. Concluding remarks

The present paper reports a simple method for the chemical synthesis of two nitroso derivatives, which were characterized electrochemically in different electrolytic media.

Also, the one-electron reduction product, the nitroso radical anion, from both nitroso derivatives was characterized by UV–vis and EPR spectroscopy in aprotic media.

Reduction mechanisms were confirmed by a simulation process using CV simulation software. Results from these experiments demonstrated that the proposed mechanisms are consistent with those obtained by simulation.

Acknowledgements

This work has been supported by Grants 8000016 from FONDECYT and DID-University of Chile.

References

[1] C. Karakus, P. Zuman, J. Electrochem. Soc. 142 (1995) 4020.
[2] M.R. Asirvatham, M.D. Hawley, J. Electroanal. Chem. 57 (1974) 179.
[3] P. Zuman, B. Shah, Chem. Rev. 94 (1994) 1621.
[4] J. Luis, J.A. Núñez-Vergara, C. Olea-Azar Squella, S. Bollo, P.A. Navarrete-Encina, J.C. Sturm, Electrochim. Acta 45 (2000) 3555.
[5] P.B. Ayscough, F.P. Sargent, R. Wilson, J. Chem. Soc. B. (1966) 903.
[6] C.J.W. Gutch, W.A. Waters, Proc. Chem. Soc. (1964) 230.
[7] E.J. Geels, R. Konaka, G.A. Russell, Chem. Commun. (1965) 13.
[8] G.A. Russell, E.J. Geels, J. Am. Chem. Soc. 87 (1965) 122.
[9] M. Nakata, A. Nasuda-Kouyama, Y. Isogai, Sh. Kanegasaki, T. Iisuka, J. Biochem. 122 (1997) 188.
[10] A. Nasuda-Kouyama, M. Nakata, T. Iisuka, Y. Isogai, J. Biochem. 122 (1997) 550.
[11] H.G. Boit, Belstein Handbuch der Organischen Chemie, 3rd ed., Springer-Verlag, Berlin, 1964.
[12] R.S. Nicholson, I. Shain, Anal. Chem. 36 (1964) 1406.
[13] G. Bontempelli, F. Magno, G. Mozzochin, R. Seeger, Ann. Chim. 79 (1989) 138.
[14] L.J. Núñez-Vergara, J.C. Sturm, A. Alvarez-Lueje, C. Olea-Azar, C. Sunkel, J.A. Squella, J. Electrochem. Soc. 146 (1999) 1478.
[15] A.G. Asuero, M.A. Herrador, A.G. González, Talanta 40 (1993) 479.
[16] A.J. Bard, L.R. Faulkner, Electrochemical Methods. Fundamentals and Applications, Wiley, New York, 1990 (p. 160).
[17] M. Olmstead, R. Hamilton, R.S. Nicholson, Anal. Chem. 41 (1969) 260.
[18] B. Kwiatek, M. Kalinowski, J. Electroanal. Chem. 226 (1987) 61.
[19] S. Bollo, L.J. Núñez-Vergara, J.A. Squella, Bol. Soc. Chil. Quím. 44 (1999) 67.
[20] M. Ohmstead, R.S. Nicholson, Anal. Chem. 41 (1969) 862.